

# Temporal variability in the thermal requirements for vegetation phenology on the Tibetan plateau and its implications for carbon dynamics

Zhenong Jin<sup>1</sup> · Qianlai Zhuang<sup>1,2</sup> · Jeffrey S. Dukes<sup>3,4</sup> · Jin-Sheng He<sup>5,6</sup> · Andrei P. Sokolov<sup>7</sup> · Min Chen<sup>1</sup> · Tonglin Zhang<sup>8</sup> · Tianxiang Luo<sup>9</sup>

Received: 11 October 2015 / Accepted: 3 July 2016  
© Springer Science+Business Media Dordrecht 2016

**Abstract** Static thermal requirements ( $T_{req}$ ) are widely used to model the timing of phenology, yet may significantly bias phenological projections under future warming conditions, since recent studies argue that climate warming will increase  $T_{req}$  for triggering vegetation phenology. This study investigates the temporal trend and inter-annual variation of  $T_{req}$  derived from satellite-based spring and autumn phenology for the alpine and temperate vegetation on the Tibetan Plateau from 1982 to 2011. While we detected persistent warming in both spring and autumn across this time period, we did not find a corresponding long-term increase in  $T_{req}$  for

---

**Electronic supplementary material** The online version of this article (doi:10.1007/s10584-016-1736-8) contains supplementary material, which is available to authorized users.

---

✉ Qianlai Zhuang  
qzhuang@purdue.edu

<sup>1</sup> Department of Earth, Atmospheric, and Planetary Sciences, Purdue University, CIVIL 550 Stadium Mall Drive, West Lafayette, IN 47907-2051, USA

<sup>2</sup> Department of Agronomy, Purdue University, West Lafayette, Indiana 47907, USA

<sup>3</sup> Department of Forestry and Natural Resources, Purdue University, West Lafayette, IN 47907, USA

<sup>4</sup> Department of Biological Sciences, Purdue University, West Lafayette, IN 47907, USA

<sup>5</sup> Key Laboratory of Adaptation and Evolution of Plateau Biota, Northwest Institute of Plateau Biology, Chinese Academy of Sciences, Xining 810008, China

<sup>6</sup> Department of Ecology, College of Urban and Environmental Sciences, Peking University, Beijing 100871, China

<sup>7</sup> Joint Program on the Science and Policy of Global Change, Massachusetts Institute of Technology, Cambridge, MA 02139, USA

<sup>8</sup> Department of Statistics, Purdue University, West Lafayette, IN 47907, USA

<sup>9</sup> Key Laboratory of Tibetan Environment Changes and Land Surface Processes, Institute of Tibetan Plateau Research, Chinese Academy of Sciences, Beijing 100085, China

most of the study area. Instead, we found a substantial interannual variability of  $T_{req}$  that could be largely explained by interannual variations in other climatic factors. Specifically, the number of chilling days and fall temperature were robust variables for predicting the dynamics of  $T_{req}$  for spring onset and autumn senescence, respectively. Phenology models incorporating a dynamic  $T_{req}$  algorithm performed slightly better than those with static  $T_{req}$  values in reproducing phenology derived from SPOT-VGT NDVI data. To assess the degree to which  $T_{req}$  variation affects large-scale phenology and carbon cycling projections, we compared the output from versions of the Terrestrial Ecosystem Model that incorporated static and dynamic  $T_{req}$  values in their phenology algorithms. Under two contrasting future climate scenarios, the dynamic  $T_{req}$  setting reduced the projected growing season length by up to 1–3 weeks by the late twenty-first century, leading to a maximum reduction of 8.9 % in annual net primary production and ~15 % in cumulative net ecosystem production for this region. Our study reveals that temporal dynamics of  $T_{req}$  meaningfully affect the carbon dynamics on the Tibetan Plateau, and should thus be considered in future ecosystem carbon modeling.

## 1 Introduction

The term “phenology” refers to the timing of recurring biological phases, such as the unfolding of leaves in spring and senescence in the autumn (Linderholm 2006). During the past few decades, phenological events in temperate zones have generally advanced in spring and postponed in autumn in response to the land surface warming and changing precipitation regimes (Linderholm 2006; Jeong et al. 2012). Altered phenology will in turn feed back to the global climate system (Penuelas and Filella 2009), since plant phenology is a fundamental regulator of the annual rhythms of carbon, water and energy exchanges between the land surface and the atmosphere (Jeong et al. 2012; Cleland et al. 2012; Richardson et al. 2013). Improving the modeling of phenological events is therefore an important step in reducing the uncertainty in projections made by ecosystem models (Richardson et al. 2012).

Large-scale phenology is often simulated by process-based models that explicitly describe known or assumed cause–effect relationships between phenological processes and driving environmental factors (Jeong et al. 2012; Richardson et al. 2013). Temperature has long been recognized as the most important factor in determining the timing of vegetation onset, development and senescence (Körner 2007). The fulfillment of a thermal requirement ( $T_{req}$ ), by reaching either a specified value of a moving average temperature or a cumulative heat sum (i.e. sum of growing degree days, GDD), will trigger a phenological event in these models. For many biomes,  $T_{req}$  can be used to predict phenology because low temperatures limit cell division, cell enlargement, or cell differentiation, and hence the formation of new plant tissue (Körner 2007). Yet spatial and temporal patterns of  $T_{req}$  values are not well understood, which has hindered the development of phenology modeling as  $T_{req}$  values directly determine the simulated start and end of the growing season. Misrepresenting phenology requirements in models can dramatically skew the simulated start/end of the growing season, and hence the quantification of terrestrial ecosystem carbon budgets (Jeong et al. 2012; Richardson et al. 2012).

Spatially,  $T_{req}$  is often treated as a species- or plant functional type (PFT)-specific parameter, resulting in use of a single value across a large geographic area (Sitch et al. 2003; Krinner et al. 2005; Richardson et al. 2012). Several recent studies have shown that substantial variations in  $T_{req}$  exist on continental, regional and even local spatial scales (Eccel et al.

2009; Piao et al. 2011; Shen et al. 2012; Fu et al. 2014). This spatial heterogeneity is likely because plant communities can adjust to the local climate (Körner 2007) through genetic evolution, local adaptation or fast species turnover. Consequently, vegetation in warmer areas requires higher thermal thresholds for the onset of growth and senescence compared to vegetation in cooler areas (Eccel et al. 2009; Bennie et al. 2010; Piao et al. 2011; Shen et al. 2012). However, such adaptation mechanisms are rarely captured in ecosystem models (but see ORCHIDEE, in which  $T_{req}$  for C3 grasses at a given place is linearly interpolated between 185 °Cd and 400 °Cd based on the multiannual mean temperature (Krinner et al. 2005)).

The temporal dynamics of  $T_{req}$  have received even less attention. Assuming that space-for-time substitution applies, one might then expect that  $T_{req}$  values will increase over time as mean temperatures warm. For example, Piao et al. (2011) argued that 1 °C of warming would increase the thermal threshold for vegetation green-up by about 0.8 °C on the Tibetan Plateau (TP). However, the rates of  $T_{req}$  changes in response to warming vary across different vegetation types in China's temperate zone (Shen et al. 2012). If  $T_{req}$  co-varies with climatic changes in a similar way to what Shen et al. (2012) showed across space, we would expect plant phenology to become less sensitive to warming as thermal requirements change (Eccel et al. 2009). In that case, the use of static thresholds for predicting future phenology would become unreliable, because the thresholds will increasingly overestimate the temperature sensitivity of phenological responses. Research that characterizes the rates and consequences of  $T_{req}$  dynamics under a changing climate can thus reduce uncertainty in phenology modeling and improve terrestrial carbon quantification.

In this study, we further investigated the temporal trend and climate-dependency of  $T_{req}$  for alpine and temperate ecosystems on the TP (Fig. 1a), by analyzing the temporal trend of  $T_{req}$  derived from satellite-derived vegetation phenology. We chose the TP as our study area for three reasons. First, plants in this area are primarily constrained by temperature and highly sensitive to regional warming (Piao et al. 2011). Second, a consistent spatial pattern of higher  $T_{req}$  for places with higher mean annual temperature exists (Fig. S1), making the TP well suited for studying temporal dynamics in  $T_{req}$ . Finally, major ecosystems on the TP are important to the current and future regional carbon balance (Zhuang et al. 2010; Piao et al. 2012). To examine the sensitivity of phenology and carbon cycling predictions to temporal dynamics in  $T_{req}$  for the TP during the twenty-first century, we implemented a dynamic  $T_{req}$  algorithm into the Terrestrial Ecosystem Model (TEM), and compared outputs from the default and modified TEM to identify the consequences of the dynamic algorithm for projections of regional net primary production (NPP) and net ecosystem production (NEP) during the twenty-first century.

## 2 Materials and methods

### 2.1 Phenology and thermal threshold

We derived phenological metrics such as start and end of growing seasons (SOS/EOS) for alpine ecosystems on the TP (Fig. 1) from the third generation Global Inventory Monitoring and Modeling System (GIMMS) normalized difference vegetation index (NDVI) data (Tucker et al. 2005) for years 1982–1999, and the NDVI product of Système Pour L'Observation de la Terre (SPOT) 4 and 5 satellites for years 2000–2011. We did not use the GIMMS NDVI3g

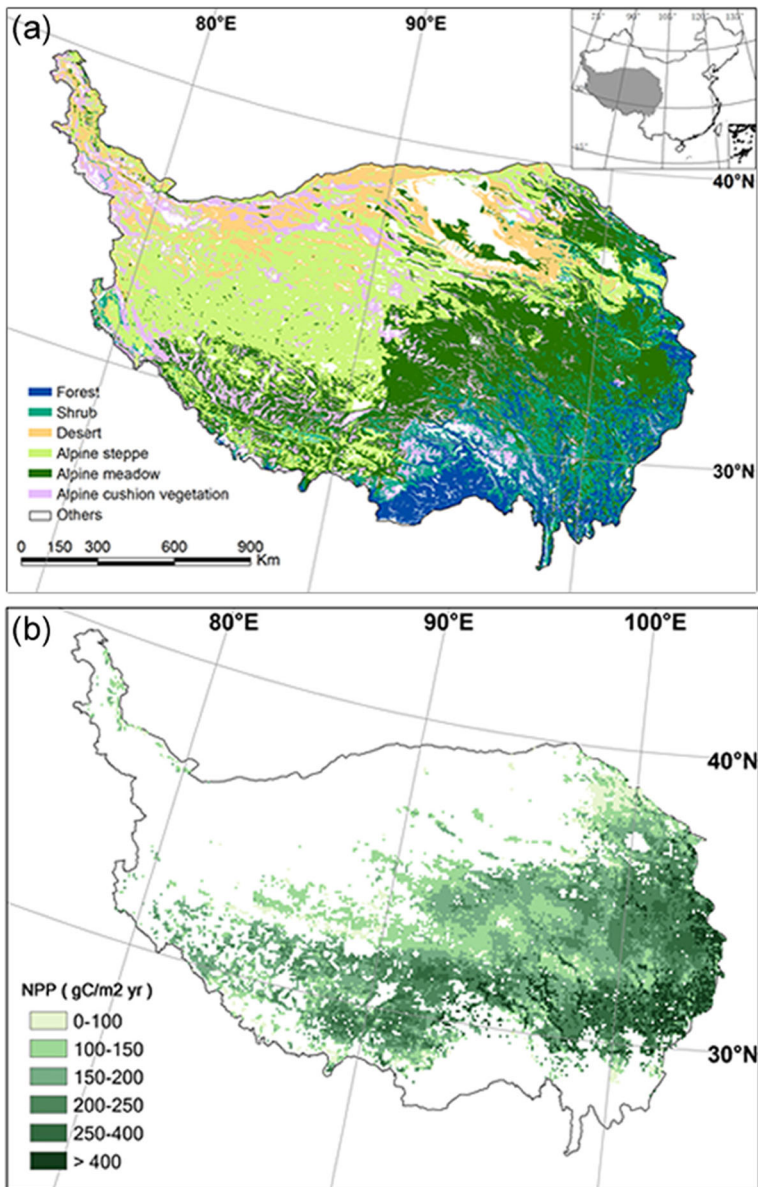


**Fig. 1** Study area information: **a** Vegetation map of the Tibetan Plateau, redrawn from the Vegetation Map of China (Chinese Academy of Science 2001). **b** Simulated annual net primary production (NPP) with units of  $\text{g C m}^{-2} \text{ year}^{-1}$  during the 2000s

data for the whole study period, because it has been criticized for low data quality at this region during the most recent decade (Zhang et al. 2013). The biweekly GIMMS NDVI3g data has a spatial resolution of  $8 \text{ km} \times 8 \text{ km}$ . The SPOT NDVI data has an original spatial resolution of  $1 \text{ km} \times 1 \text{ km}$ , but was aggregated into  $8 \text{ km} \times 8 \text{ km}$  for consistency. The effects of satellite change, sensor degradation and atmospheric contaminations have been removed from the raw data of both satellites following standard preprocessing

procedures (Maisongrande et al. 2004; Tucker et al. 2005). To further reduce the data noise, we removed all pixels with mean annual NDVI values less than 0.1, which were considered as snow cover, water body, bare soil, or extremely sparse vegetation (Piao et al. 2011). Pixels labeled as “others” in the vegetation map were masked out (Fig. 1a). We also applied the Savitzky-Golay Filter with a window length of 5 to the NDVI time series as a way of denoising.

To determine the date of vegetation onset and senescence for each pixel, we first fitted a polynomial equation to the multi-year averaged NDVI time series to get the seasonal curve following Piao et al. (2011). From the seasonal curve, we calculated the NDVI threshold for spring onset and autumn senescence following (Yu et al. 2010):

$$NDVI_{\text{threshold}} = NDVI_{\text{min}} + [NDVI_{\text{max}} - NDVI_{\text{min}}] \times NDVI_{\text{ratio}} \quad (1)$$

where  $NDVI_{\text{min}}$  is the average of February and March rather than the minimum of the seasonal curve;  $NDVI_{\text{max}}$  is the annual maximum;  $NDVI_{\text{ratio}}$  is 0.2 for SOS and 0.6 for EOS. The derived  $NDVI_{\text{threshold}}$  was then used to determine SOS and EOS for each year. We randomly subset 10 % of the SPOT NDVI data and left out for validating the new phenology algorithm (see section 2.4).

$T_{\text{req}}$  for spring onset was calculated using the GDD method:

$$GDD = \sum_{t_0}^{\text{SOS}} \max(T - T_{\text{base}}, 0) \quad (2)$$

in which  $t_0$  and  $T_{\text{base}}$  are the starting date and base temperature for GDD accumulation, respectively. Here,  $t_0$  was prescribed as January 1st and  $T_{\text{base}}$  was 0 °C. It should be noted that both 0 °C and 5 °C are widely used for  $T_{\text{base}}$  when calculating GDD (Eccel et al. 2009; Jeong et al. 2013; Fu et al. 2014; Shen et al. 2015), but our preliminary analysis showed that 5 °C failed to capture the GDD signal on the central and western parts of the TP. In addition, we calculated 7-day retrospective moving average soil temperature ( $T_{\text{soil}_7}$ ) for SOS as another measure of  $T_{\text{req}}$ , given that soil temperature has been well recognized as a stable thermal indicator for alpine ecophysiology (Körner and Paulsen 2004; Körner 2007; Jin et al. 2013).  $T_{\text{req}}$  for EOS was only calculated in forms of  $T_{\text{soil}_7}$ .

## 2.2 TEM and soil temperature simulation

Soil temperature at 10 cm depth was simulated by TEM model at a spatial resolution of 8 km × 8 km for the TP from 1982 to 2011. TEM is a process-based ecosystem model designed to make daily or monthly estimations of carbon and nitrogen fluxes and pool sizes of the terrestrial biosphere by using spatially referenced information on climate, topography, soils and vegetation (Zhuang et al. 2010). The version of TEM we used here is coupled with a soil thermal model (STM) that simulates daily soil temperatures at different depths (Zhuang et al. 2001), and has been verified extensively to give reasonable estimation of soil temperature and permafrost dynamics in alpine and high latitude regions (Zhuang et al. 2001; Tang and Zhuang 2011; Jin et al. 2013). Zhuang et al. (2010) parameterized TEM for major ecosystems on the TP, and examined the effect of permafrost dynamics on carbon cycling for the past century. The same version was later applied by Jin et al. (2013) to investigate the relationship between soil temperature and

vegetation phenology on the TP. More detailed model description and information on data preparation was given in Methods S1.

### 2.3 Trend and partial correlations

We calculated the historical trend in  $T_{req}$  of both SOS and EOS at each pixel for three periods, namely, 1981–2011, 1981–1999 and 2000–2011. Our preliminary analysis showed that the historical trend was similar between certain vegetation types (i.e. forest and shrub, steppe and desert, meadow and alpine cushion). Therefore, we aggregated forest and shrub as “wood”, which is characterized by having aboveground buds during the dormant season; aggregated steppe and desert as “steppe”, which can be viewed as dry grassland; and aggregated meadow and alpine cushion as “meadow”, which is moister than steppe. Trend analysis was then performed for each aggregated vegetation type.

To evaluate the climate dependency of  $T_{req}$ , we investigated a number of environmental variables based on existing literature. For spring, candidate variables include mean spring air temperature, mean preseason air temperature, mean spring and preseason soil temperature, cumulative spring and preseason precipitation, number of chilling days (NCD). For autumn, candidate variables include mean preseason air and soil temperature, cumulative summer precipitation and summer maximum weekly vapor pressure deficit. Abbreviations and definitions for these climate variables are listed in Table S1. We included NCD because several recent studies have emphasized the negative correlation between chilling and GDD requirements (Jeong et al. 2013; Fu et al. 2014; Shen et al. 2015). We calculated NCD as number of days when 7-day moving average temperature drops below 0 °C since September 1st in last year. The impacts of climate variables on  $T_{req}$  were quantified using the partial correlation analysis by setting phenological metrics (i.e. SOS and EOS) as the control variable. This partial regression helped to remove the covariation among multiple climatic factors, and also partly reduced the uncertainty in metrics that were dependent on SOS or EOS. For instance, if SOS is negatively biased, the corresponding GDD and temperature threshold will also be negatively biased. All the data processing and analysis were performed using R statistical software.

### 2.4 Updated phenology algorithm and TEM applications

In TEM, the impact of vegetation phenology on gross primary production (GPP) is modeled as a scalar function,  $f(\text{phenology})$ , between 0 and 1 (Methods S2). This study added soil thermal constraints on the phenological process as a sub-scalar of thermal free percentage  $f(T_{req})$ :

$$f(T_{req}) = \begin{cases} 0 & \text{if } T_{\text{indicator}} \leq T_{req} \\ 1 & \text{if } T_{\text{indicator}} > T_{req} \end{cases} \quad (3)$$

where  $T_{\text{indicator}}$  is daily-updated  $GDD$  (calculated by Eqn-2) during spring and  $T_{\text{soil}_7}$  during autumn, and  $T_{req}$  is the corresponding threshold (i.e.  $GDD_{req}$  for SOS and  $T_{\text{soil}_7, req}$  for EOS). The updated  $f(\text{phenology})$  now becomes a product of the original scalar and  $f(T_{req})$ . To mimic the empirical relations between thermal requirement and climatic factors,  $T_{req}$  was reset for each growing season according to changes in NCD



and preseason air temperature (see results for variable selection). For a given year  $t$ , the spring  $T_{req}$  was calculated as:

$$GDD_{req}(t) = GDD_{req}(t-1) - \beta_1 \times \Delta NCD(t) \quad (4)$$

in which  $\Delta NCD$  is the difference in NCD between the current and previous year, and will modify  $GDD_{req}$  in a rate of  $\beta_1$  ( $^{\circ}\text{C}/\text{day}$ ). Similarly, fall  $T_{req}$  was calculated as:

$$T_{soil7,req}(t) = T_{soil7,req}(t-1) + \beta_2 \Delta T_{Fall}(t) \quad (5)$$

where  $\Delta T_{Fall}$  is the change in fall soil temperature compared to the previous year, and will adjust  $T_{soil7,req}$  in a rate of  $\beta_2$  ( $^{\circ}\text{C}/^{\circ}\text{C}$ ). Values of  $GDD_{req}$  and  $T_{soil7,req}$  for the first year were derived from historical mean. The prognostic SOS and EOS models were validated using the left-out 10 % SPOT-VGT phenology data in section 2.1 for the period 2000–2011.

To quantify the sensitivity of future phenology and carbon projections to changes in  $T_{req}$ , we ran TEM for the twenty-first century with both static ( $\beta_1$  and  $\beta_2 = 0$ ) and dynamic ( $\beta_1$  and  $\beta_2 \neq 0$ ) thermal requirements. The value of  $\beta_1$  and  $\beta_2$  was derived from the partial regression analysis for each aggregated vegetation type (Table S2), and was essential for the sensitivity test. Vegetation-specific parameters for TEM were determined by calibrating the model output to best fit the fluxes and pool sizes of field measurements (Methods S3). Two future climate scenarios with a daily time step from 2001 to 2100 were generated by the MIT's Integrated Global Systems Model (IGSM) (Sokolov et al. 2009; Webster et al. 2012): a stabilization case of policy control (PC) on greenhouse gas emissions and a business-as-usual case of no-policy control (NPC). Under PC scenario, the atmospheric  $\text{CO}_2$  concentration rises to 478.55 ppm by volume (ppmv) by the end of twenty-first century, and is accompanied by 1.8  $^{\circ}\text{C}$  regional warming; under NPC, these values are 903.55 ppmv and 4.7  $^{\circ}\text{C}$  warming. The original data with 0.5 degree cells were resampled to 8 km  $\times$  8 km using the inverse distance weighting method. We ran TEM with static and dynamic  $T_{req}$  under each of the two emissions scenarios, producing a total of 4 projected future trajectories.

## 3 Results

### 3.1 Historical trend of thermal requirement

During 1982–2011, both spring and autumn temperature on the TP had significant warming trends of 0.4–0.5  $^{\circ}\text{C}/\text{decade}$  across all vegetation types (Table 1). However,  $T_{req}$  for SOS and EOS did not consistently increase over this period. For spring, only GDD in the steppe showed a significant trend of 1.13  $^{\circ}\text{C}/\text{yr}$ . (Fig. 2a). The 30-year  $T_{Threshold}$  was almost zero (Fig. 2c), suggesting moving-averaged temperature was indeed a stable thermal indicator within a time window of few decades. For autumn, no meaningful trend in  $T_{Threshold}$  was observed for wood, while significant increasing trends were detected for both steppe (0.37  $^{\circ}\text{C}/\text{decade}$ ) and meadow (0.23  $^{\circ}\text{C}/\text{decade}$ ) (Fig. 2e). When splitting the study period into 1982–1999 and 2000–2011, no significant trend changes (change in coefficient sign) were observed (Table 1), indicating that the 30-year temporal trend in  $T_{req}$  was robust. Spatially, only 22 % of the total pixels had a significant change in spring GDD (Fig. 2b), with large increases ( $>2$   $^{\circ}\text{C}/\text{yr}$ ) mainly taking place in the northeast of the TP. In contrast, only 14 % of total pixels had a significant

**Table 1** Vegetation-specific coefficients of linear regressions between the thermal requirements or environment variables and corresponding times. See Table S1 for variable definitions

	1982–2011			1982–1999			2000–2011		
	Wood	Steppe	Meadow	Wood	Steppe	Meadow	Wood	Steppe	Meadow
Spring									
GDD	0.18	1.13***	0.24	-0.17	1.53*	0.57	0.11	1.74*	1.05
TTholdS	-0.007	0.006	-0.01	-0.019	0.015	-0.013	-0.007	0.015	-0.012
NCD	-0.45***	-0.46***	-0.36***	-0.96***	-0.62***	-0.69***	-0.36*	-0.29	-0.32
TSpring	0.042***	0.044***	0.039**	0.11***	0.082**	0.066***	0.07*	0.063*	0.061*
TPre	0.011	0.046**	0.016*	0.01	0.044	0.017	0.02	0.15*	0.077*
PrecSpr	0.21	-0.093	-0.037	0.87	0.23	0.45	-1.23	-1.01*	-0.69
PrecPre	-0.07	0.043	-0.087	0.15	0.13	0.07	-1.68*	0.19	-0.78
Fall									
TTholdF	0.0	0.037***	0.023**	-0.004	0.010	0.004	-0.008	0.044*	0.038
TFall	0.052***	0.044***	0.043***	0.03	0.034	0.024	0.031*	0.069***	0.037*
PrecSum	0.15	1.35***	1.19*	-0.25	2.72***	1.13	1.23	-0.35	1.7*
MaxVPD	0.0	-0.004	0.007	0.0	-0.016*	0.009	-0.04	-0.01	-0.03

Statistical significance: “\*\*\*\*”,  $P < 0.001$ ; “\*\*\*”,  $P < 0.01$ ; “\*”,  $P < 0.5$

change in terms of *TTholdS*, and no apparent spatial aggregation was identified (Fig. 2d). For *TTholdF*, 21 % of the total study area had a significant change, in which most of the changes were positive ( $>0.5$  °C/decade) and occurred in steppe and meadow ecosystems (Fig. 2f).

### 3.2 Relationship between thermal requirement and climate factors

Although trend analysis suggested that only a small portion of the vegetation community had statistically significant changes in  $T_{req}$  over the 30-year study period, the inter-annual variation of these  $T_{req}$  were indeed substantial (Fig. 2). Noticing that several climate variables that can potentially regulate  $T_{req}$ , such as chilling days, spring and fall temperature and summer precipitation changed significantly for 1982–2011 (Table 1), we further questioned whether the inter-annual variability of  $T_{req}$  was induced by variation in year-to-year weather or simply a result of uncertainty from phenology extraction.

For the spring, strong partial correlations were identified between GDD and a portion of candidate climate variables after setting SOS as the control variable (Fig. 3). Partial correlations were significantly negative between GDD and NCD for all vegetation types, in which the strongest correlation occurred in steppe ( $\rho = -0.81$ ,  $P < 0.001$ ) and followed by wood and meadow. GDD was also significantly correlated with temperature (i.e. *TPre* or *TSpring*), with the strength of partial correlation mostly similar to that between GDD and NCD except much higher in wood (Fig. 3a). The effect of precipitation was to reduce the GDD requirement, especially in the dry ecosystem of steppe, but none of these negative partial correlations from different vegetation types were significant. The partial correlations between *TTholdS* and climate variables were mostly non-significant, except for the significant negative correlations with NCD ( $\rho = -0.57$ ,  $P < 0.001$ ) and *PrecPre* ( $\rho = -0.43$ ,  $P = 0.023$ ) observed in steppe. Based on the partial correlation analysis, we believe chilling fulfillment is a good explanatory variable for the inter-annual variability in the GDD requirement. First, NCD incorporates some



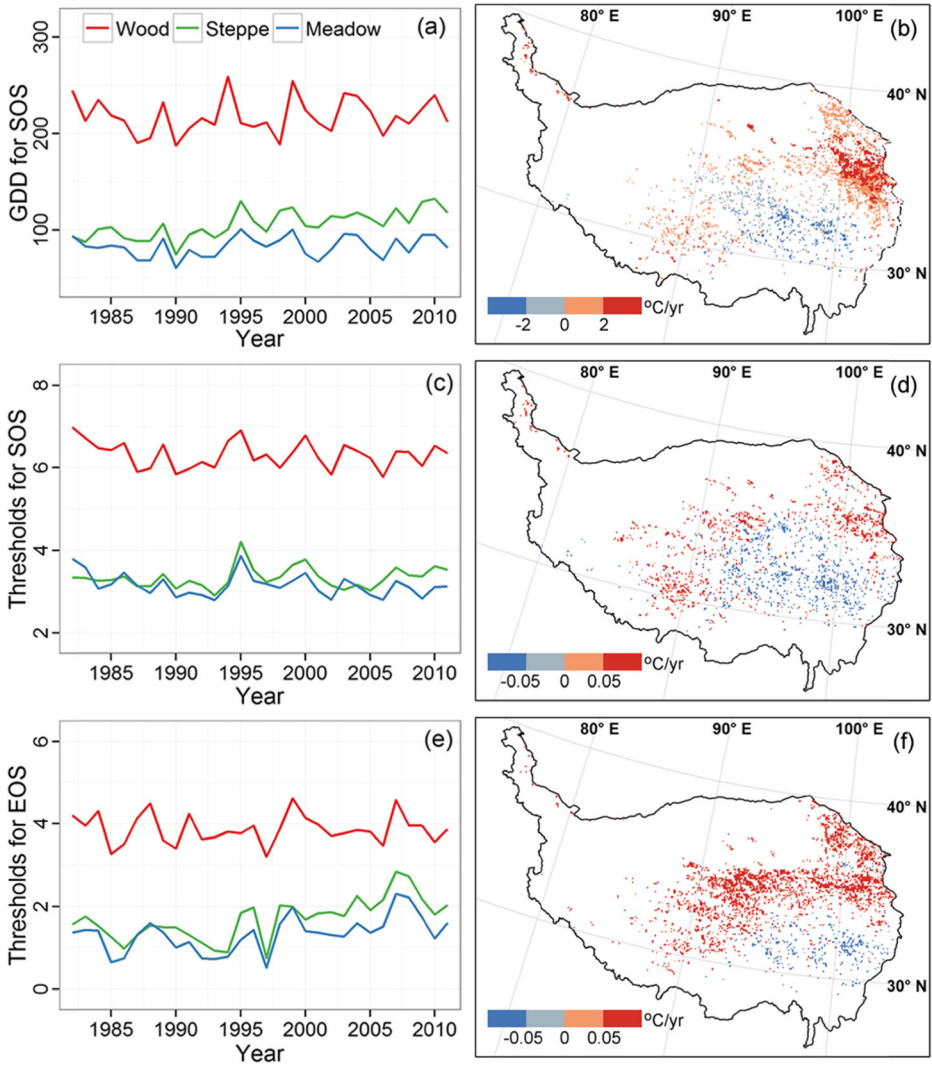
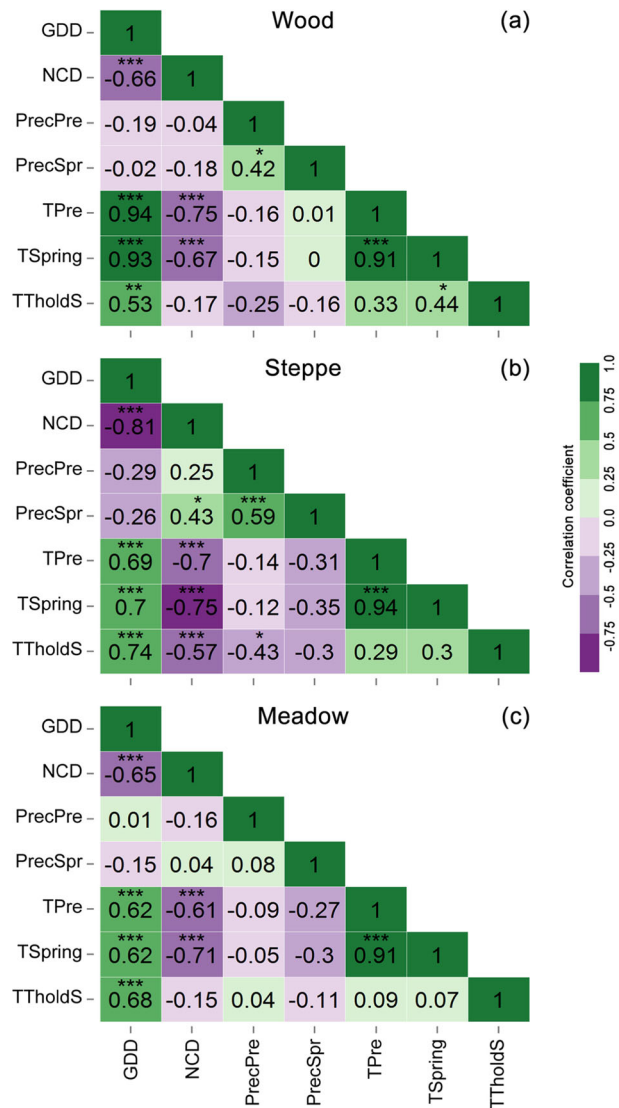


**Fig. 2** Averaged temporal dynamics of thermal requirement for each vegetation type and spatial patterns from 1982 to 2011. **a** and **b**: GDD requirement for SOS; **c** and **d**: Moving average temperature threshold for SOS; **e** and **f**: threshold for EOS. For the spatial map, only pixels with significant change ( $\alpha = 0.05$ ) in thermal requirement are shown

of the variation in two of the other explanatory variables,  $TP_{Pre}$  and  $TS_{Spring}$ , because these thermal metrics were all highly correlated. Second, NCD is more robust and easy to implement because its calculation in most cases is not dependent on the SOS (SOS normally happened after  $T_{air} > 0$ , a time point when the accumulation of chilling days is already over). For the autumn,  $T_{ThresholdF}$  was significantly correlated with  $TP_{Pre}$  for all vegetation types (Fig. 4), and the strongest partial correlation also occurred in steppe ( $\rho = 0.81, P < 0.001$ ). Summer precipitation unexpectedly increased  $T_{ThresholdF}$ , although the partial correlation was only significant in steppe ( $\rho = 0.64, P < 0.001$ ). We speculate that the positive correlation between precipitation and  $T_{req}$  might occur because wetter conditions shall boost summer growth leading to greater

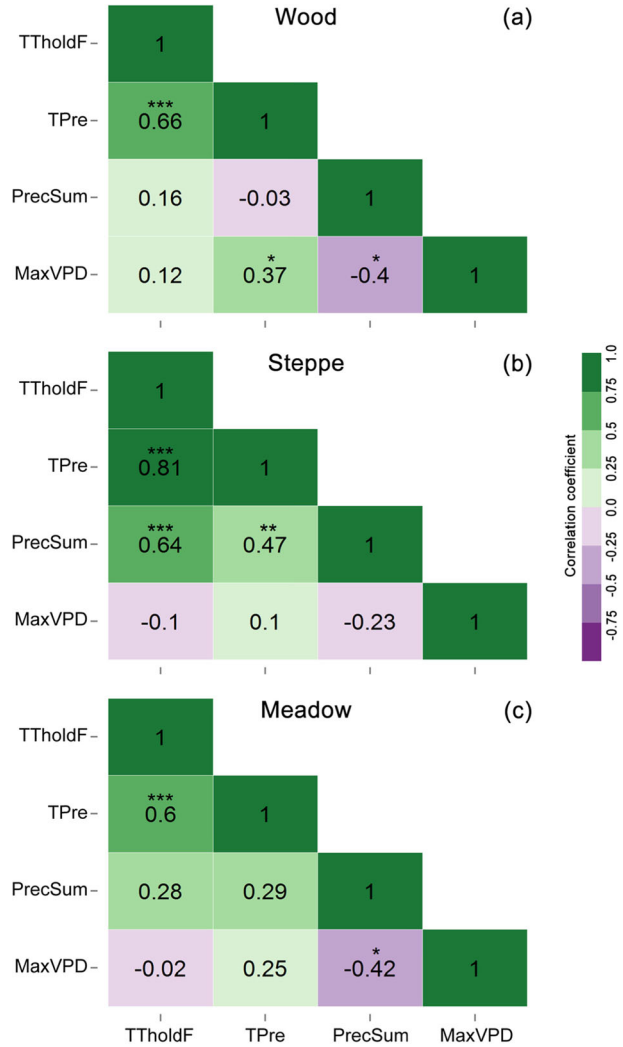
**Fig. 3** Vegetation-specific mean partial correlation between thermal requirement for spring onset and environmental factors after setting SOS as the control variable. See Table S1 for variable definition. Statistical significance: \*,  $P < 0.05$ ; \*\*,  $P < 0.01$ ; \*\*\*,  $P < 0.001$



water or nutrient depletion and hence early growth termination. *MaxVPD*, an indicator supposed to capture both high temperature and the lag effect of water deficit, was not related to the temporal variation in *TThresholdF*.

Based on the coefficients of partial correlations, we developed a set of dynamic  $T_{req}$  for each vegetation type (Table S2). New phenology algorithms were validated against the left-out 10 % SPOT-VGT NDVI data. Compared with remotely sensed spring onset, simulated SOS for the years 2000–2011 had much higher root mean square errors (RMSE) of 6–16 days using vegetation-specific GDD requirements than using localized parameters (Fig. S2a). Differences between simulations with static and dynamic  $T_{req}$  were small (0.5 to 2.1 days), but the latter consistently had smaller biases in terms of RMSE. Model-predicted EOS in general had a smaller RMSE than that of SOS (Fig. S2b). Simulations with localized *TThresholdF* reduced

**Fig. 4** Vegetation-specific mean partial correlation between thermal requirement for autumn senescence and environmental factors after setting EOS as the control variable. See Table S1 for variable definition. Statistical significance: \*,  $P < 0.05$ ; \*\*,  $P < 0.01$ ; \*\*\*,  $P < 0.001$



RMSE to less than 5 days, compared with 6–15 days of bias from models that assign a vegetation-specific parameter of  $T_{req}$ . Furthermore, RMSE was 1–2 days smaller for simulations with dynamic  $T_{req}$  than those with localized but static  $T_{req}$ .

### 3.3 Simulated future phenology and carbon cycling

Modifications in the phenology algorithm meaningfully affected projections of both phenology and carbon cycling. SOS and EOS for the twenty-first century differed substantially among four simulations (Fig. 5a, b). SOS advanced less under the PC scenario than the NPC scenario. The smallest advancements came with dynamic  $T_{req}$  under PC (slope = 0.3 days/decade,  $P < 0.001$ ), while the greatest advancement occurred in the simulation with static  $T_{req}$  under NPC, in which SOS advanced by 2.1 days/decade ( $P < 0.001$ ). Similarly, simulated EOS was delayed as much as 1.9 days/decade ( $P < 0.001$ ) with fixed  $T_{req}$  under NPC but only 0.2 days/

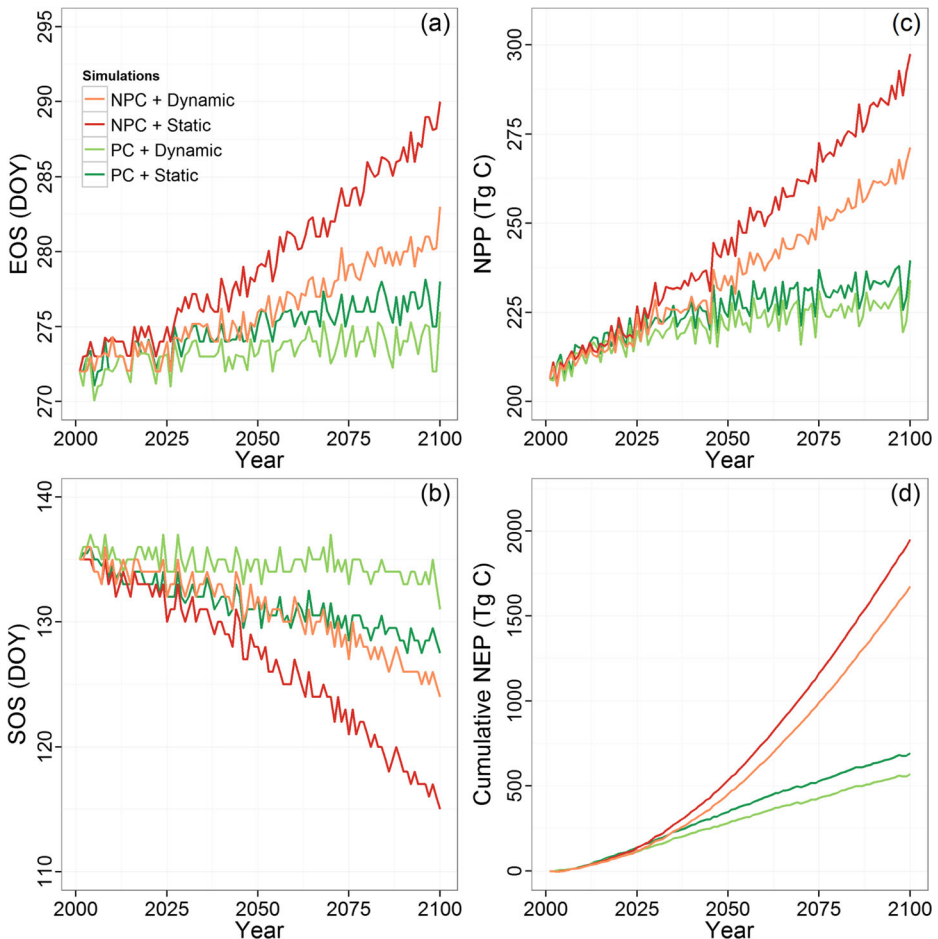


**Fig. 5** Projections of (a) end of growing season, (b) start of growing season, (c) net primary production and (d) cumulative net ecosystem production for the study area during the twenty-first century. Simulations are based on two future climate scenarios of policy control and no-policy control on greenhouse gas emissions combined with assumptions of static and dynamic thermal requirement

decade ( $P < 0.001$ ) with dynamic  $T_{req}$  under PC (Fig. 5a). Growing season length extended by 1 to 6 weeks, depending on assumptions about  $T_{req}$  and the climate scenario. In general, higher emission scenarios will enlarge the difference between projections with static and dynamic  $T_{req}$ .

For carbon modeling, our simulated baseline annual NPP for the 2000s was comparable with other modeling or inventory-based estimations for major biomes on the TP (Table S3). The estimated mean annual NPP density ( $187 \text{ g C m}^{-2} \text{ yr}^{-1}$ ) falls in the range of other regional studies ( $90\text{--}330 \text{ g C m}^{-2} \text{ yr}^{-1}$ ). Spatially, NPP density was higher in eastern and southeastern parts of the TP, and lower towards the northwest (Fig. 1b). Decadal mean annual NPP was projected to increase from  $211.1 \text{ Tg C yr}^{-1}$  in the 2000s up to  $233.6 \text{ Tg C yr}^{-1}$  in the 2090s under PC, and from  $209.8$  to  $263.9\text{--}287.6 \text{ Tg C yr}^{-1}$  under NPC (Fig. 5c). The relative effect on NPP of using a dynamic  $T_{req}$  was 2.7 % under PC and 8.9 % under NPC. Our estimated mean annual NEP ( $3.1 \text{ Tg C yr}^{-1}$ ) for the 2000s was close to zero, suggesting alpine

ecosystems on the TP have been nearly carbon neutral in recent years. This estimate is consistent with Fang et al. (2010), who found neither biomass nor soil C stock in China's grasslands changed significantly during the past 20 years. Cumulative NEP was 569–691 Tg C at the end of the twenty-first century under PC and 1674–1950 Tg C under NPC (Fig. 5d). Using a dynamic  $T_{req}$  reduced cumulative NEP projections by 17.7 % under PC and 14.2 % under NPC.

## 4 Discussion

### 4.1 Understanding thermal requirement dynamics

Studies of temporal variation in  $T_{req}$  have not drawn much attention until recent years (Eccel et al. 2009; Fu et al. 2015), and the causes thus remain elusive. Ecological consequences of such variation may be important, as we found a relative difference of 8.9 % in NPP and a ~ 15 % relative difference in NEP through scenario simulations. Whether  $T_{req}$  truly operate through cumulative heat demand or environmental cues of a favored leaf-out condition still needs to be clarified with additional study. If  $T_{req}$  is viewed as heat demand, it may shift because changes in other climate factors could compensate or moderate the demand via complex feedbacks. A number of such regulating factors have been proposed, among which the roles of chilling (Körner 2007; Eccel et al. 2009; Jeong et al. 2013; Fu et al. 2014, 2015; Shen et al. 2015) and precipitation (Fu et al. 2014; Shen et al. 2015) have been repeatedly emphasized. In our study, we also identified significant partial correlations between the strength of chilling and GDD, and showed that phenology models with a dynamic GDD requirement simulate observations better than the default model. However, our analysis did not support a role of precipitation in shaping the GDD requirement. The use of total precipitation data in our study, without discrimination between rainfall and snow could be one reason. While hypotheses have put forward to explain how water availability can adjust phenological thermal requirements (Fu et al. 2015), our mechanistic understanding of this issue remains rudimentary, and the topic deserves further investigation.

If  $T_{req}$  is viewed as an environmental cue rather than an indicator of heat demand, its changes over time are more likely a result of acclimation, genetic evolution or phenotypic plasticity determined by local environmental cues (Diez et al. 2012). Evolution is thought to be a slow process, but evolutionary rates may largely depend on the costs associated with having the “wrong” phenological response at a given time (Pau et al. 2011). Species with short generation times and large population sizes (e.g. annual grassland species on the TP) have greater potential to evolve under rapid climate change (Hoffmann and Sgro 2011). Species in variable habitats may be more sensitive to climatic cues, and hence more capable of adjusting their growth strategy to maximize survival and reproduction (Pau et al. 2011). Under selection pressures, the ability of an individual to shift  $T_{req}$  could be further explained as an inherited self-protection mechanism against being overly sensitive to climatic variation (Bennie et al. 2010).

### 4.2 Uncertainties and implications

This study is among the first to use long-term NDVI datasets to investigate the temporal trend of phenological  $T_{req}$  for alpine vegetation. However, a few limitations of this study should be mentioned, and potential solutions are discussed.

First, there are several sources of data uncertainties. Although we have applied several steps to reduce the noise in the NDVI time-series during preprocessing, phenological results must be interpreted in view of the biweekly temporal resolution for GIMMS or 10 days for SPOT-VGT (Zhu et al. 2012). The choice of  $NDVI_{ratio}$  to determine phenological metrics also brings uncertainty (White et al. 2009; Shen et al. 2015). Compared with observational phenology data, RMSE under our  $NDVI_{ratio}$  is 10.6 days for SOS and 13.5 days for EOS (Yu et al. 2010). In addition, downscaling coarse climate data into finer resolution is another source of data uncertainty (Frauenfeld et al. 2005), but can be reduced if the density of meteorological stations increases in the future (Jin et al. 2013). Essentially, any improvements in remote sensing data, methods for extracting phenological metrics, or reanalysis products will greatly improve our ability to quantify the temporal trend of thermal requirement and its climatic causes.

Second, while our analysis mainly focused on temperature, fulfillment of chilling, and precipitation, other climatic factors including photoperiod (Jeong et al. 2012), light intensity (Fu et al. 2015), and snowmelt (Inouye and Wielgolaski 2013) should be further examined in future studies. In temperate grassland, photoperiod plays a secondary role after other climatic constraints (Migliavacca et al. 2011), and is more often linked with flowering rather than leaf out. Therefore, we believe photoperiod does not currently constrain the phenology of the alpine ecosystem on the TP, but may become a limiting factor in the future. Light intensity (often measured by downward shortwave irradiance) has minor effects on the large portion of our study area that is covered by steppe and meadow and dominated by plant species whose buds remain belowground during dormancy. Although snowmelt can affect phenology in alpine regions (Migliavacca et al. 2011; Richardson et al. 2013), we believe the impact of snow is reduced by using average NDVI of February and March as the  $NDVI_{min}$ . Moreover, our results still held when we increased the spring  $NDVI_{ratio}$  from 0.2 to 0.3 (data not shown), indicating the impact of snow melting is small.

Third, by using remote sensing data, we could only test for apparent changes in heat requirement for the whole community within each pixel, and thus could not isolate responses of individual plants or even species. Evidence shows that species with different phylogenetic origins usually have different thermal requirements for triggering phenology (Bennie et al. 2010; Diez et al. 2012), and late season species often show larger shifts in thermal requirements than early season groups in response to the ongoing warming (Fu et al. 2015). We believe such a mechanism is unlikely to operate in our study, because there was no evidence of fast year-to-year species turnover in alpine ecosystems on the TP, but vegetation dynamics should be taken into account when phenology models are applied to regions in which the flora is undergoing changes. To fully untangle the complex pattern of changes in thermal requirements at the community level, additional observations and well-designed warming manipulation experiments are required (Richardson et al. 2013).

## 5 Conclusion

In this study, we investigated the temporal trend and inter-annual variability of  $T_{req}$  for alpine and temperate vegetation phenology on the Tibetan Plateau. Our analysis uncovered only a weak trend in  $T_{req}$  over time, even as the climate warmed dramatically over the same period. A more significant trend was observed in steppe and meadow, which have faster potential



turnover of individuals and species than woody ecosystems. We found that  $T_{req}$  was correlated with the inter-annual variation of several climate factors, indicating that this indicator for thermal demand can adjust quickly to shifting climate conditions. The number of chilling days and fall temperature were robust predictors for the  $T_{req}$  of spring and autumn, respectively. Projected future phenology and regional-scale carbon cycling over the twenty-first century were sensitive to the choice of static or dynamic  $T_{req}$  in the phenology model. Our results indicated that the temporal dynamics of  $T_{req}$  were different from its spatial patterns, and would have meaningful impacts on regional carbon cycling. We expect that the analysis presented in this study can be applied in other temperate and arctic regions where warming is expected to be more dramatic in the future. Identifying and understanding the mechanisms through which climatic factors co-vary with thermal requirement can improve projections of plant phenology in the ecosystem models that use PFTs to represent the vegetation community, and further reduce the uncertainty in future carbon cycle projections.

**Acknowledgments** We thank Zhiyao Tang, Shilong Piao and Yue Shi for helpful comments on the manuscript. This research is supported with a NSF project (DEB- #0919331), the NSF Carbon and Water in the Earth Program (NSF-0630319), the NASA Land Use and Land Cover Change program (NASA-NNX09A126G), Department of Energy (DE-FG02-08ER64599), and the NSF Division of Information & Intelligent Systems (NSF-1028291), funded to Q.Z.

## Reference

- Bennie J, Kubin E, Wiltshire A, Huntley B, Baxter R (2010) Predicting spatial and temporal patterns of bud burst and spring frost risk in north-west Europe: the implications of local adaptation to climate. *Glob Chang Biol* 16(5):1503–1514
- Chinese Academy of Sciences (2001) *Vegetation Atlas of China*. Science Press, Beijing
- Cleland EE, Allen JM, Crimmins TM, et al. (2012) Phenological tracking enables positive species responses to climate change. *Ecology* 93:1765–1771
- Diez JM, Ibáñez I, Miller-Rushing AJ, et al. (2012) Forecasting phenology: from species variability to community patterns. *Ecol Lett* 15:545–553
- Eccel E, Rea R, Caffarra A, Crisci A (2009) Risk of spring frost to apple production under future climate scenarios: the role of phenological acclimation. *Int J Biometeorol* 53:273–286
- Fang J, Yang Y, Ma W, Mohammad A, Shen H (2010) Ecosystem carbon stocks and their changes in China's grasslands. *Science China Life Sciences* 53:757–765
- Frauenfeld OW, Zhang T, Serreze MCCD (2005) Climate change and variability using European Centre for Medium-Range Weather Forecasts reanalysis (ERA-40) temperatures on the Tibetan Plateau. *J Geophys Res Atmos* 110. doi:10.1029/2004JD005230
- Fu YH, Piao S, Vitasse Y, et al. (2015) Increased heat requirement for leaf flushing in temperate woody species over 1980–2012: effects of chilling, precipitation and insolation. *Glob Chang Biol* 21:2687–2697
- Fu YH, Piao S, Zhao H, Jeong S-J, Wang X, Vitasse Y, Ciais P, Janssens IA (2014) Unexpected role of winter precipitation in determining heat requirement for spring vegetation green-up at northern middle and high latitudes. *Glob Chang Biol* 20:3743–3755
- Hoffmann AA, Sgro CM (2011) Climate change and evolutionary adaptation. *Nature* 470(7335):479–485
- Inouye DW, Wielgolaski FE (2013) Phenology at high altitudes. In: *Phenology: an integrative environmental science*. Springer, Netherlands, pp 249–272
- Jeong S-J, Medvigy D, Shevliakova E, Malyshev S (2013) Predicting changes in temperate forest budburst using continental-scale observations and models. *Geophys Res Lett* 40:359–364
- Jeong S-J, Medvigy D, Shevliakova E, Malyshev SCG (2012) Uncertainties in terrestrial carbon budgets related to spring phenology. *J Geophys Res Biogeosci* 117. doi:10.1029/2011JG001868
- Jin Z, Zhuang Q, He J-S, Luo T, Shi Y (2013) Phenology shift from 1989 to 2008 on the Tibetan Plateau: an analysis with a process-based soil physical model and remote sensing data. *Clim Chang* 119:435–449
- Körner C (2007) *Significance of temperature in plant life*. Plant Growth and Climate Change. Blackwell Publishing Ltd, pp. 48–69
- Körner C, Paulsen J (2004) A world-wide study of high altitude treeline temperatures. *J Biogeogr* 31(5):713–732

- Krinner G, Viovy N, de Noblet-Ducoudré N, et al. (2005) A dynamic global vegetation model for studies of the coupled atmosphere-biosphere system. *Glob Biogeochem Cycles* 19. doi:10.1029/2003GB002199
- Linderholm HW (2006) Growing season changes in the last century. *Agric For Meteorol* 137:1–14
- Maisongrande P, Duchemin B, Dedieu G (2004) VEGETATION/SPOT: an operational mission for the Earth monitoring; presentation of new standard products. *Int J Remote Sens* 25(1):9–14
- Migliavacca M, Galvagno M, Cremonese E, et al. (2011) Using digital repeat photography and eddy covariance data to model grassland phenology and photosynthetic CO<sub>2</sub> uptake. *Agric For Meteorol* 151:1325–1337
- Pau S, Wolkovich EM, Cook BI, Davies TJ, Kraft NJB, Bolmgren K, Betancourt JL, Cleland EE (2011) Predicting phenology by integrating ecology, evolution and climate science. *Glob Chang Biol* 17:3633–3643
- Peñuelas J, Filella I (2009) Phenology feedbacks on climate change. *Science* 324(5929):887–888
- Piao S, Cui M, Chen A, Wang X, Ciais P, Liu J, Tang Y (2011) Altitude and temperature dependence of change in the spring vegetation green-up date from 1982 to 2006 in the Qinghai-Xizang Plateau. *Agric For Meteorol* 151:1599–1608
- Piao S, Tan K, Nan H, Ciais P, Fang J, Wang T, Vuichard N, Zhu B (2012) Impacts of climate and CO<sub>2</sub> changes on the vegetation growth and carbon balance of Qinghai–Tibetan grasslands over the past five decades. *Glob Planet Chang* 98–99:73–80
- Richardson AD, Anderson RS, Arain MA, et al. (2012) Terrestrial biosphere models need better representation of vegetation phenology: results from the North American Carbon Program Site Synthesis. *Glob Chang Biol* 18:566–584
- Richardson AD, Keenan TF, Migliavacca M, Ryu Y, Sonnentag O, Toomey M (2013) Climate change, phenology, and phenological control of vegetation feedbacks to the climate system. *Agric For Meteorol* 169:156–173
- Shen M, Piao S, Cong N, Zhang G, Jassens IA (2015) Precipitation impacts on vegetation spring phenology on the Tibetan Plateau. *Glob Chang Biol* 21:3647–3656
- Shen M, Tang Y, Chen J, Yang W (2012) Specification of thermal growing season in temperate China from 1960 to 2009. *Clim Chang* 114:783–798
- Sitch S, Smith B, Prentice IC, et al. (2003) Evaluation of ecosystem dynamics, plant geography and terrestrial carbon cycling in the LPJ dynamic global vegetation model. *Glob Chang Biol* 9:161–185
- Sokolov AP, Stone PH, Forest CE, et al. (2009) Probabilistic Forecast for Twenty-First-Century Climate Based on Uncertainties in Emissions (Without Policy) and Climate Parameters. *J Clim* 22:5175–5204
- Tang J, Zhuang Q (2011) Modeling soil thermal and hydrological dynamics and changes of growing season in Alaskan terrestrial ecosystems. *Clim Chang* 107:481–510
- Tucker CJ, Pinzon JE, Brown ME, et al. (2005) An extended AVHRR 8-km NDVI dataset compatible with MODIS and SPOT vegetation NDVI data. *Int J Remote Sens* 26:4485–4498
- Webster M, Sokolov A, Reilly J, et al. (2012) Analysis of climate policy targets under uncertainty. *Clim Chang* 112:569–583
- White MA, Beurs D, Kirsten M, et al. (2009) Intercomparison, interpretation, and assessment of spring phenology in North America estimated from remote sensing for 1982–2006. *Glob Chang Biol* 15(10):2335–2359
- Yu H, Luedeling E, Xu J (2010) Winter and spring warming result in delayed spring phenology on the Tibetan Plateau. *Proc Natl Acad Sci* 107:22151–22156
- Zhang G, Zhang Y, Dong J, Xiao X (2013) Green-up dates in the Tibetan Plateau have continuously advanced from 1982 to 2011. *Proc Natl Acad Sci* 110(11):4309–4314
- Zhu W, Tian H, Xu X, Pan Y, Chen G, Lin W (2012) Extension of the growing season due to delayed autumn over mid and high latitudes in North America during 1982–2006. *Glob Ecol Biogeogr* 21(2):260–271
- Zhuang Q, Romanovsky VE, McGuire AD (2001) Incorporation of a permafrost model into a large-scale ecosystem model: Evaluation of temporal and spatial scaling issues in simulating soil thermal dynamics. *J Geophys Res-Atmos* 106(D24):33649–33670
- Zhuang Q, He J, Lu Y, Ji L, Xiao J, Luo T (2010) Carbon dynamics of terrestrial ecosystems on the Tibetan Plateau during the twentieth century: an analysis with a process-based biogeochemical model. *Glob Ecol Biogeogr* 19:649–662